HEFAT2014
10th International Conference on Heat Transfer, Fluid Mechanics and Thermodynamics
14 – 26 July 2014
Orlando, Florida

LATTICE MONTE CARLO SIMULATION OF THERMAL CONDUCTIVITY IN COMPOSITE MATERIALS

Zhe Cheng[b], Zhichun Liu[a]*, Dongdong Wang[a], Yingshuang Wang[a], Jinguo Yang[a], Wei Liu[a]*
[a] School of Energy and Power Engineering,
Huazhong University of Science and Technology,
Wuhan 430074,
China,
[b] 2010 Black Engineering Building
Department of Mechanical Engineering
Iowa State University
Ames, IA 50011
(E-mail: zcliu@hust.edu.cn, w_liu@hust.edu.cn)

ABSTRACT

This paper addresses the numerical simulation of thermal conductivity of composite material. A Lattice Monte Caro method is used in the analysis of two-dimensional two-component models with different inclusions, including circular inclusion, elliptical inclusion, square inclusion, random-generated circular inclusions. Through simulation on these models, relationships among phase fraction of low conductivity phase (B phase), ratio of thermal conductivities of two phases (B and A) and relative effective thermal conductivities are obtained. Also, thermal conductivity of porous silicon with porosity of 26% is predicted and excellent agreements are achieved when compared with experimental results. Finally, research on thermal conductivity of sintered porous nickel is carried out. Microstructure image which is obtained with scanning electron microscope (SEM) is digitized by image processing method. The results exhibit a good agreement with experimental results in literature.

INTRODUCTION

A composite is a material having two or more distinct constituents or phases [1], which processes many excellent thermal and mechanical properties, such as large heat capacity, significantly-reduced or enhanced thermal conductivity, and high strength. Due to these fascinating properties, in the past few decades composite material has been extensive utilized as thermoelectric material [2-4], heat sink[5], heat insulation, phase change energy storage material [6-9], fiber reinforced composite material [10-11].

As an important parameter of composite material, thermal conductivity has been a hot research topic recently, which is no longer an inherent property of the material itself after the appearance of composite [12]. However, experimental measurement on thermal conductivity of composite has many disadvantages, for instance, high-cost and time consuming. Thus, methods of predicting thermal conductivity of composite have been developing rapidly recently.

Ben-Amoz [13] discussed effective thermal properties of two-phase solids. Rio [14] proposed approximate calculation formula for the conductivity of a two-component material based on reciprocity theorem and the results agree well with experimental results. When phase fraction is smaller than 0.1 or larger than 0.9, good results would be obtained using Maxwell equation. Samantray[15] studied the effective thermal conductivity of two phase composite and put forward that different models should be employed based on effective thermal conductivity of matrix phase and dispersed phase. Wang [16] simulated the structure of multiphase composite with random generation method and then they obtained the effective thermal conductivity after using Lattice Boltzmann to solve energy transport equation.

In this work, a recent developed Lattice Monte Carlo (LMC) is used to simulate thermal conductivity of two-phase composite. LMC method is a simulation method based on Fick's Law or Einstein equation which has been proven as an excellent method to solve a variety of heat and mass diffusion problems [17-20].

METHOD

In Lattice Monte Carlo method, physical model is scaled into lattice and thermal diffusion is simulated by virtual particle. This kind of particle represents extreme small but finite amount of energy which would jump from one node in the lattice to another. Its jump direction is selected randomly and whether the particle would jump is constricted by jump probability . Jump probability is selected according to thermal diffusion of

constituents or phases. Two random numbers are generated to select a particle and its jump direction. The jump probability is calculated according to target node and origin node of the thermal diffusion, which would be compared with a random number. If jump probability is larger than this random number, the particle jumps successfully and coordinates would be updated and calculation time would increase by one time unit. Otherwise only calculation time increases.

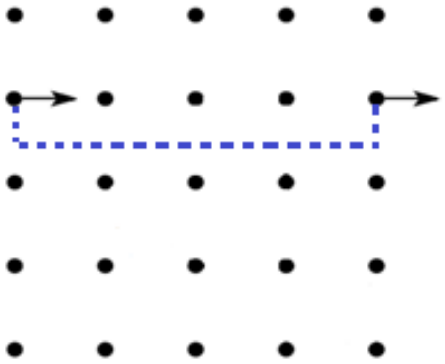

Fig.1 Periodic boundary condition for LMC

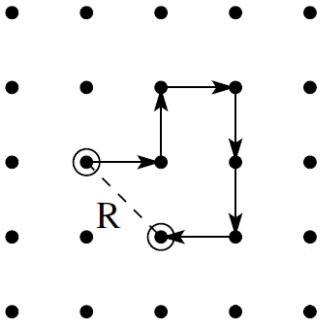

Fig.2 Schematic of displacement for a particle after 6 times jumping in 2D 5x5 lattice

100x100x100

In the simulation process, a large number of particles would be released to the lattice and calculation time should be large enough to guarantee accuracy. There are 100x100 lattices in present computation domain, that is, there are 1 million particles in our calculation. In order to guarantee accuracy, each particle must at least jump 50,000 times at each shifting. Moreover, in order to eliminate stochastic error, the calculation is repeated 10 times for each working condition. Additionally, periodic boundary condition is employed in this paper, that is, when a particle passes through one face of the calculation domain, it reappears on the opposite face with the same direction, just as shown in Fig.1. Finally, displacement of each particle R would be obtained to determine displacement square, and Fig.2 is schematically shown the displacement for a particle after 6 times jumping in 2D 5x5 lattice. Then the mean of displacement square under large particle number N_p can be calculated. Einstein equation (1) is used to calculate thermal diffusion D_{eff} .

$$D_{\text{eff}} = \frac{\left\langle R^2 \right\rangle}{2 \cdot \text{d} \cdot \text{t}} \qquad (1)$$

Where, D_{eff} is effective diffusion coefficient; $\left\langle R^2 \right\rangle$ is mean of displacement square under large particle number N_{p} ; d represents dimension（d=1, 2, 3）; here d equals 2 for two dimension; t is time unit, and here is total times of particle jumping..

Then we can obtain effective thermal conductivity after knowing effective density and effective heat capacity of composite. For simplification, we let $\rho_i = C_i = 1$. To improve accuracy, every case in this paper is calculated ten times and the mean of these values are obtained.

RESULTS AND DISCUSSION

In literature [21], case of Fig.5 in chapter3.2 is that circular inclusion is located in the middle of square lattice. To justify accuracy, we conducted a same simulation. The results are compared with that in the literature, just as Fig.3 shown. It can be seen that the two curves coincide, which means our simulation has excellent accuracy.

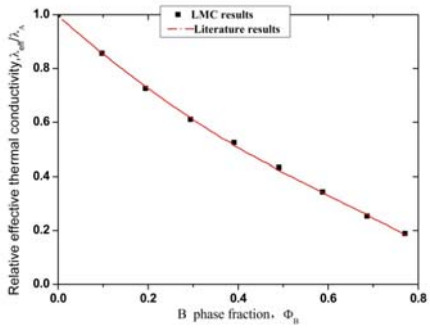

Fig.3 Relative effective thermal conductivity and B phase fraction when $\lambda_B / \lambda_A = 0.1$

Different composites have different microstructures and microstructures, for example shape and size, exert a significant effect on their thermal conductivity. Thus, different inclusions, including circular, elliptical, square, random-generated circular ones, are studied to explore effect of phase fraction on relative effective thermal conductivities. Relationships between relative effective thermal conductivity and phase fraction with various shape inclusions are obtained. Meanwhile, effect of ratio of BA phase thermal conductivity on relative effective thermal conductivity is considered.

Fig.4 indicates the effect of B phase fraction on relative effective thermal conductivity when ratio of BA phase thermal conductivities λ_B/λ_A is 0.1、0.01、0.001. It is shown that relative effective thermal conductivity deceases with increase of B phase fraction and the curves of three relative effective thermal conductivities coincide when B phase fraction ranges from 0 to 0.3. The reason is that ratio of two phases thermal conductivities has little effect on relative effective thermal conductivity when doping amount is not so large. When B phase fraction rises, influence of inclusion becomes dominant increasingly. Ratio of phase fractions affects relative effective thermal conductivity increasingly. The decrease speed of composite with $\lambda_B / \lambda_A = 0.1$ is smaller than its counterparts of composite with $\lambda_B / \lambda_A = 0.01$ and 0.001. When B phase fraction reaches $\pi / 4$, namely 0.7854, circular inclusion divides matrix material into four parts. Relative effective thermal conductivity would decrease significantly in this situation.

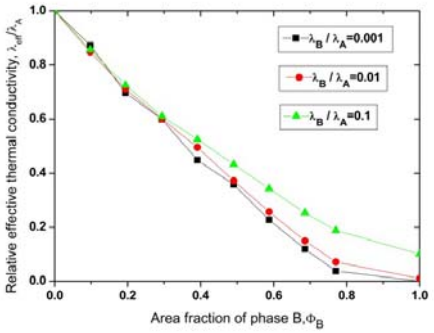

Fig.4. Relative effective thermal conductivity and B phase fraction with various ratios of thermal conductivity

As shown in Fig.4, ratio of major axis and minor axis of the ellipse is 2. When B phase fraction ranges from 0 to 0.1, the three curves coincide. This range is smaller than that of circular inclusion because inclusion would divide matrix material into two parts with a smaller B phase fraction. Additionally, effect of ratio of BA phase thermal conductivities appears at a smaller B phase fraction. Relative effective thermal conductivity with $\lambda_B / \lambda_A = 0.1$ is larger than those with $\lambda_B / \lambda_A = 0.01$ and 0.001 from where B phase fraction is 0.1.

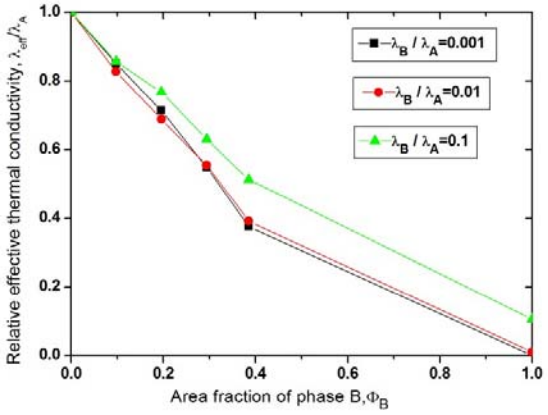

Fig.4. Relative effective thermal conductivity and B phase fraction with various ratios of thermal conductivity

To further explore the effect of inclusion dividing matrix on relative effective thermal conductivity, ellipse inclusion model with constant major axis and mutative minor axis is built.

Simulation of relative effective thermal conductivity is performed when B phase fraction ranges from0.1 to $\pi/4$.

We can see from Fig.4, ratio of BA thermal conductivities would affect relative effective thermal conductivity significantly when B phase fraction is 0.1. The relative effective thermal conductivity with $\lambda_B/\lambda_A=0.1$ would be 0.1 larger than those of the other two. Compared with ellipse with ratio of major axis and minor axis of 2, relative effective thermal conductivity decreases more when B phase fraction changes from 0 to 0.1. Result with circular inclusion decreases by 0.13, and result with ellipse with ratio of major axis and minor axis of 2 falls by 0.16 while result with another ellipse goes down by 0.23. When $\lambda_B/\lambda_A=0.01$ and 0.001, this change becomes 0.34. One reason may be that the inclusion divides matrix material into halves; then vertical particle would get caught in inclusion and mean of particle displacement square would decrease significantly.

When B phase fraction is between 0.1 and $\pi/4$, relative effective thermal conductivity exhibits a linear relationship with B phase fraction and relative effective thermal conductivities with $\lambda_B/\lambda_A=0.1$, 0.01 and 0.001 fall evenly with slope of -0.86.

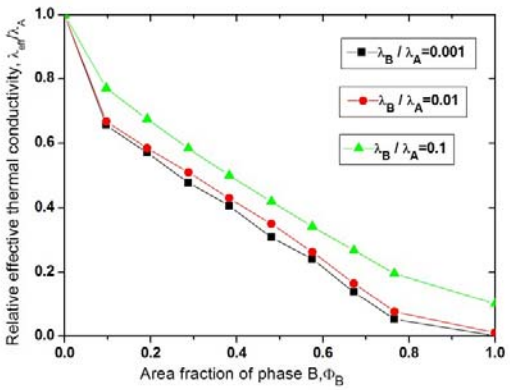

Fig.4. Relative effective thermal conductivity and B phase fraction with various ratios of thermal conductivity

As Fig.5 shown, relative effective thermal conductivity changes evenly. Relative effective thermal conductivity curves with $\lambda_B/\lambda_A=0.01$ and 0.001 almost coincide, which indicates that change of λ_B/λ_A exerts little influence on relative effective thermal conductivity when λ_B/λ_A is smaller than 0.01.

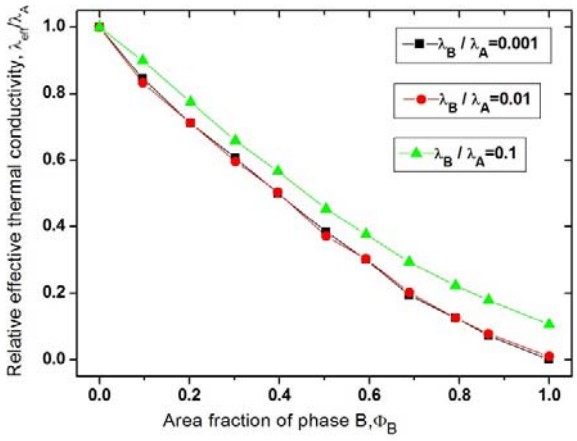

Fig.5. Relative effective thermal conductivity and B phase fraction with various ratios of thermal conductivity

2.2.4 Model with random-generated circular inclusions

To simulate the randomness of particle's size and position in composite, circular inclusions are generated randomly by computer. It can be seen from Fig.6 that eight inclusions are generated in 100x100 lattices. The circle center positions and radii are generated randomly. B phase fractions in Fig.6 from left to right are 0.1, 0.3496 and 0.6136, respectively. Here we calculated cases with B phase fraction changing from0.1 to 0.6136， meanwhile effect of ratio of BA thermal conductivity on relative effective thermal conductivity is also studied.

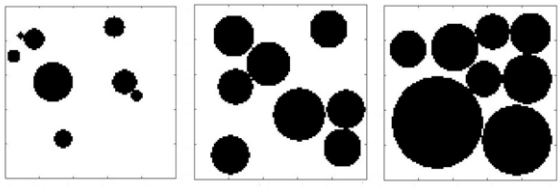

Fig.6. Model with random-generated circular inclusions

As Fig.7 shown, X axis is logarithmic coordinate. When $\lambda_B/\lambda_A>0.1$, λ_B/λ_A has an apparent effect on relative

effective thermal conductivity while this effect disappear when $\lambda_B / \lambda_A < 0.01$. Relative effective thermal conductivity decreases with increase of B phase fraction evenly.

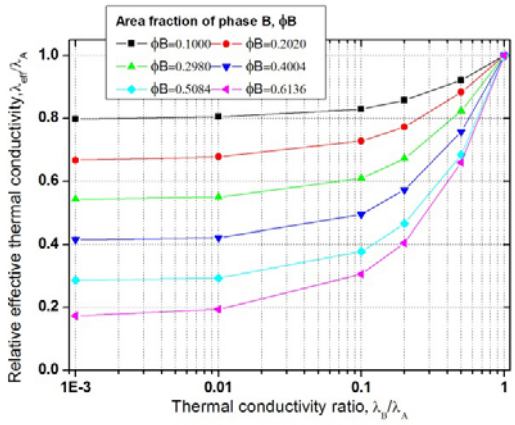

Fig.7. Relative effective thermal conductivity and ratio of BA thermal conductivity with different B phase fraction

Fig.8 depicts the relationship of relative effective thermal conductivity and B phase fraction with different λ_B / λ_A. Composite's relative effective thermal conductivity exhibits a linear relationship with B phase fraction, namely relative effective thermal conductivity decreases when B phase fraction increases. The larger B phase fraction is, the more significant effect λ_B / λ_A has on relative effective thermal conductivity, making relative effective thermal conductivity to decrease more. The reason is that when B phase accounts for a large proportion of composite, change of thermal conductivity of dominant part would significantly affect thermal conductivity of composite if λ_B / λ_A changes.

For $\lambda_B / \lambda_A = 0.01$ and 0.001, relative effective thermal conductivity decreases to 0.2 when B phase fraction is0.6136. Also, it decreases to 0.3 in case of $\lambda_B / \lambda_A = 0.1$. Relative effective thermal conductivity decreases significantly through adding inclusions into matrix material.

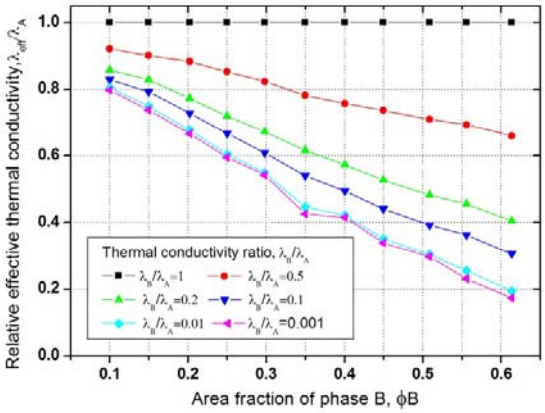

Fig.8. Relative effective thermal conductivity and B phase fraction with different ratios of BA thermal conductivity

2.3 Thermal conductivity of porous composite

2.3.1Thermal conductivity of porous silicon

When bulk silicon is made into porous silicon, phonon in porous material would reflect or refract on the surface of cavity, which results in the decrease of mean free path of phonon and then the decrease of thermal conductivity. At the same time, porous silicon's electrical conductivity changes little from bulk silicon to porous silicon, so thermoelectric efficiency would be greatly enlarged. In this case, prediction of thermal conductivity of porous silicon is meaningful and critical. Table1 gives parameters which would be used in calculation.

Table1：physical parameters of bulk silicon

	Density（Kg/m^3）	Heat capacity（J/(Kg*K)）	Thermal conductivity（W/（m*k））
Silicon（300K）	2329	705	148

Compared with silicon's thermal conductivity, air's thermal conductivity is negligible. Also, radiation can be neglected when temperature is lower than ambient. Finally, convective

heat transfer in small volume can be ignored. Thus, boundary condition of porous silicon's cavity wall can be simplified as adiabatic boundary, which means phonons only transport in silicon material. When phonons move to cavity wall, they would be reflected back. Based on Einstein Equation, diffusion coefficient of porous silicon (D_{eff}) can be obtained by LMC simulation.

$$D_{Si} = \frac{\lambda_{Si}}{\rho_{Si} \cdot C_{Si}}, \quad D_{eff} = \frac{\lambda_{eff}}{\rho_{eff} \cdot C_{eff}} \qquad (2)$$

According to formula (2), we can get the following formula:

$$\lambda_{eff} = \lambda_{Si} \cdot (1 - \phi_B) \cdot \frac{D_{eff}}{D_{Si}} \qquad (3)$$

Where, D_{si} is thermal diffusion coefficient of bulk silicon, λ_{si} is thermal conductivity of bulk silicon, ϕ_B refers to porosity of porous silicon.

The porous silicon's porosity that this paper is used is 26%. Models with circular, rectangular, ellipse random-generated circular inclusions are simulated and porous silicon's relative effective thermal conductivity is got. Relative effective thermal conductivity is defined as porous silicon's thermal conductivity divided by bulk silicon's thermal conductivity at a certain temperature. The results are shown as Fig.9.

We can see from Fig.9, rectangle, random-generated circle, circle, ellipse represent LMC results with temperature in the range of 125K to 300K. Russell and Eucken stand for the results in literature [22], which are obtained using Russell Formula、Maxwell-Eucken Formula. 10um represents experimental results in literature [22]. As shown in Fig.9, all four LMC results are closer to experimental results than those of empirical formula（Russell Formula、Maxwell-Eucken Formula）. Notably, results of models with circle and ellipse inclusions almost coincide with experimental results.

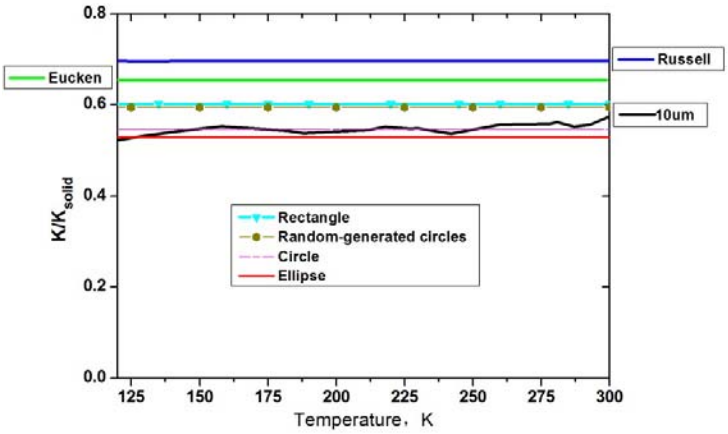

Fig.9. Porous silicon's relative effective thermal conductivity and temperature

2.3.2 Thermal conductivity of sintered porous nickel

Fig.10 is the SEM microstructure image of sintered porous silicon. The white part is nickel framework while the black part is air.

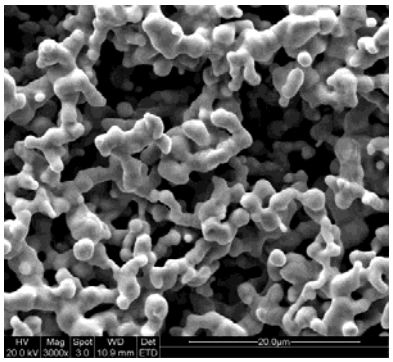

Fig.10. SEM image of sintered porous nickel

The SEM image can be transferred into grayscale image by Matlab. A threshold value is set to turn grayscale image into binary image. Porosity (66%) can be measured by weighing sample. Through changing threshold value, porosity can be fit into 66%. Because periodic boundary is employed and nickel is connected in the boundary area, we define the outer boundary pixels as nickel. The binary image is as Fig.11 shown.

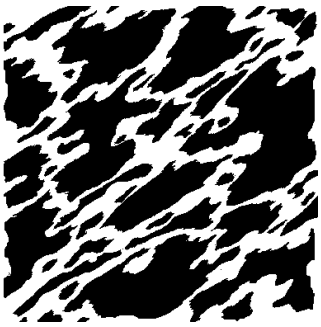

Fig.11. Binary image with porosity of 66% (400x400 pixels)

The physical parameters of nickel and air are given below.

Table 2： physical parameters of nickel

	Density （Kg/m^3）	Heat capacity （J/(Kg*K)）	Thermal conductivity （W/（m*k））
Nickel	8908	440	90.7
Air	1.184	1005	0.0257

Based on Einstein Equation, diffusion coefficient of porous nickel (D_{eff}) can be obtained by LMC simulation.

$$D_{Ni} = \frac{\lambda_{Ni}}{\rho_{Ni} \cdot C_{Ni}} \quad , \quad D_{eff} = \frac{\lambda_{eff}}{\rho_{eff} \cdot C_{eff}} \qquad (4)$$

Then, effective density and effective heat capacity can be obtained using the following formula.

$$\rho_{eff} C_{eff} = \phi_B \rho_{Ni} C_{Ni} + (1-\phi_B)\lambda_{Si}(1-\phi_B)\rho_{air} C_{air} \qquad (5)$$

Where, D_{Ni} is thermal diffusion coefficient of bulk nickel, λ_{Ni} is thermal conductivity of bulk nickel, ϕ_B is nickel's volume fraction. ρ_{Ni} and ρ_{air} are densities of nickel and air respectively; C_{Ni} and C_{air} are heat capacities of nickel and air respectively.

Then, we can get thermal conductivity of porous nickel:

$$\lambda_{eff} = \frac{\left[\phi_B \rho_{Ni} C_{Ni} + (1-\phi_B)\rho_{air} C_{air}\right]\lambda_{Si} \dfrac{D_{eff}}{D_{Si}}}{\rho_{Ni} C_{Ni}} \qquad (6)$$

Table3. LMC simulation result and experimental results in literature [23]

	LMC	Mo[23]	K& B[23]	K& B[23]
Porosity	0.613	0.557	0.61	0.53
Cavity Diameter(um)	2	2	0.65	0.52
Thermal conductivity W/(m*k)	5.188	5.90	3.73	4.08

It can be seen from Table3 that LMC simulation result reaches excellent agreement with experimental results.

3. Conclusion

This paper addresses the numerical simulation of thermal conductivity of composite material. A Lattice Monte Caro method is used in the analysis of two-dimensional two-component models with different shape inclusions, including circle, ellipse, rectangle, random-generated circle. Through LMC simulation, relationships among relative effective thermal conductivity, ratio of BA thermal conductivity, B phase fraction are obtained. Then thermal conductivities of porous silicon and sintered porous nickel are predicted and excellent agreements are achieved with experimental results.

Acknowledgement

This work was supported by the National Natural Science Foundation of China (No. 51376069, 51036003) and the National Basic Research Development Program of China (No. 2013CB228302).

REFERENCES

[1] Matthews F L, Rawlings R D. Composite materials: engineering and science[M]. Woodhead Publishing, 1999.

[2] Minnich A J, Dresselhaus M S, Ren Z F, et al. Bulk nanostructured thermoelectric materials: current research and future prospects[J]. Energy & Environmental Science, 2009, 2(5): 466-479.

[3] Chen G. Recent trends in thermoelectric materials research III[J]. Semiconductors and Semimetals, 2001, 71: 203-259.

[4] Chen G, Dresselhaus M S, Dresselhaus G, et al. Recent developments in thermoelectric materials[J]. International Materials Reviews, 2003, 48(1): 45-66.

[5] Huibin Yina, Xuenong Gaoa, Jing Dingb, Zhengguo Zhanga：Experimental research on heat transfer mechanism of heat sink with composite phase change materials. Energy Conversion and Management. 2008, 49(6), 1740–1746.

[6] Zhao H, Pokharel M, Chen S, et al. Figure-of-merit enhancement in nanostructured FeSb2− xAgx with Ag1− ySby nanoinclusions[J]. Nanotechnology, 2012, 23(50): 505402.

[7] Liu W, Lukas K C, McEnaney K, et al. Studies on the Bi2Te3–Bi2Se3–Bi2S3 system for mid-temperature thermoelectric energy conversion[J]. Energy & Environmental Science, 2013, 6(2): 552-560.

[8] Zhang Q, Wang H, Zhang Q, et al. Effect of Silicon and Sodium on Thermoelectric Properties of Thallium-Doped Lead Telluride-Based Materials[J]. Nano letters, 2012, 12(5): 2324-2330.

[9] Sharma A, Tyagi V V, Chen C R, et al. Review on thermal energy storage with phase change materials and applications[J]. Renewable and Sustainable energy reviews, 2009, 13(2): 318-345.

[10] Ku H, Wang H, Pattarachaiyakoop N, et al. A review on the tensile properties of natural fiber reinforced polymer composites[J]. Composites Part B: Engineering, 2011, 42(4): 856-873.

[11] Liao K, Schultheisz C R, Hunston D L, et al. Long-term durability of fiber-reinforced polymer-matrix composite materials for infrastructure applications: a review[J]. Journal of advanced materials, 1998, 30(4): 3-40.

[12] Chen G, Shakouri A. Heat transfer in nanostructures for solid-state energy conversion[J]. TRANSACTIONS-AMERICAN SOCIETY OF MECHANICAL ENGINEERS JOURNAL OF HEAT TRANSFER, 2002, 124(2): 242-252.

[13] Ben-Amoz M. The effective thermal properties of two phase solids[J]. International Journal of Engineering Science, 1970, 8(1): 39-47.

[14] Rio, J.A., Zimmerman, R.W., Dawe, R.A.: Formula for the conductivity of a two-component material based on the reciprocity theorem. Solid State Commun. 1998,106, 183–186

[15] Samantray, P.K., Karthikeyan, P., Reddy, K.S.: Estimating effective thermal conductivity of two-phase materials. Int. J. Heat Mass Transf. 2006,49, 4209–4219

[16] Wang, M., Pan, N.: Predictions of effective physical properties of complex multiphase materials. Mater. Sci. Eng. 2008, 63, 1–30

[17] Belova, I.V., Murch, G.E., Fiedler, T., O ¨ chsner, A.: The Lattice Monte Carlo method for solving phenomenological mass and heat transport problems. Defect Diffus. Forum 2008, 279,13–22

[18] Fiedler, Thomas, et al. "Lattice Monte Carlo and Experimental Analyses of the Thermal Conductivity of Random-Shaped Cellular Aluminum." Advanced Engineering Materials 11.10 (2009): 843-847.

[19] Belova, Irina V., et al. "The Lattice Monte Carlo method for solving phenomenological mass and thermal diffusion problems." Defect and Diffusion Forum. Vol. 279. 2008.

[20] Fiedler, Thomas, et al. "Calculation of the effective thermal conductivity in composites using finite element and Monte Carlo methods." Materials science forum. Vol. 553. Trans Tech, 2007.

[21] Belova I V, Murch G E, Fiedler T, et al. The lattice Monte Carlo method for solving phenomenological mass and heat transport problem[J]. Diffusion Fundamentals, 2007, 4: 1-23.

[22] Song D, Chen G. Thermal conductivity of periodic microporous silicon films[J]. Applied physics letters, 2004, 84(5): 687-689.

[23] Mo S, Hu P, Cao J, et al. Effective thermal conductivity of moist porous sintered nickel material[J]. International journal of thermophysics, 2006, 27(1): 304-313.